CHARACTERIZATION OF MONTMORILLONITES FROM BENTONITE DEPOSITS OF NORTH PATAGONIA, ARGENTINA: PHYSICOCHEMICAL AND STRUCTURAL PARAMETER CORRELATION

Lombardi, B.; Baschini, M.; Torres Sánchez, R.M.*

(CIMAR) Centro de Materiales Arcillosos, Fac. de Ingeniería, Universidad Nacional del Comahue, Bs. Aires 1400, (8300) Neuquén, Argentina
*(CETMIC) Centro de Tecnología de Recursos Minerales y Cerámica. Cno. Centenario y 506, CC 49, (B1897ZCA) M.B. Gonnet, Argentina. e-mail:rosats@netverk.com.ar

Received August 23, 2002. In final form: November 14, 2002

Abstract

Thirteen bentonite deposits of North Patagonia, Argentina, were characterised by chemical and differential thermal analysis (DTA), X-ray diffraction, Mössbauer spectroscopy, and Cation Exchange Capacity (CEC) and Specific Surface area (S) determinations. The chemical analysis on <2μm fraction permitted to calculate the nature and degree of isomorphic substitution (octahedral and tetrahedral). Parameters as CEC, S and thermal stability (T) (determined by DTA analyses) were correlated linearly with the degree of tetrahedral isomorphic substitution. These parameters and the mathematical models obtained could be used to predict technological uses of this mineral. Electron microscopy observation showed different modes of particle associations related also, as the precedent parameters, to the degree of tetrahedral isomorphic substitution. The adsorption on bentonite of organic pollutants was evaluated using a fungicide (Thiabendazole) employed in the same region. Fungicide adsorption increased with the degree of tetrahedral isomorphic substitution and consequently with the surface area and CEC values of the samples studied.

Resumen

Se caracterizaron trece depósitos de bentonitas de la Norpatagonia Argentina a través de análisis químicos y térmicos diferenciales (ATD), difracción de rayos X, espectroscopía Mössbauer y determinaciones de capacidad de intercambio catiónico (CIC) y de superficie específica (S). El análisis químico de la fracción <2μm permitió calcular la naturaleza y el grado de las sustituciones isomórficas (octaédricas y tetraédricas). Parámetros tales como CIC, S y temperatura de estabilidad térmica (T, determinada por ATD) se correlacionaron linealmente con el grado de sustitución isomórfica tetraédrica. Estos parámetros y los modelos matemáticos encontrados pueden ser utilizados para predecir la utilización tecnológica de este mineral. Observaciones por microscopía electrónica mostraron distintos modos de asociación de las partículas, relacionados también, al igual que los parámetros precedentes, con el grado de sustitución tetraédrica. Se evaluó la adsorción de contaminantes orgánicos utilizando un fungicida (Thiabendazole) de uso regional. Se observó un aumento de la adsorción del fungicida con el grado de sustitución tetraédrica y consecuentemente con los valores de superficie específica y CIC de las muestras empleadas.

Introduction

Montmorillonites are clay minerals broadly employed in industrial processes. These minerals stand out by some properties as great specific surface area (S) and high thermal stability (T), among others, which make them effective as adsorbents, catalytic support, for foundry materials and as viscosity modifiers.

S and T, used as technological parameters, are related to changes produced in the crystal structure by isomorphic substitutions. These isomorphic substitutions take place in both tetrahedral and octahedral layers of the mineral producing a total negative charge density in the crystal structure, which allows electrostatic interactions with positively charged molecules. Besides, some treatments, which modified the crystal structure i.e. cationic changes, thermal and mechanical treatments [1-4] can also alter technological properties such as compression strength, swelling degree, resistance to degradation, etc.

Particularly, the thermal stability of montmorillonites has been linearly correlated to the degree of isomorphic substitution [3]. In soils, with some content of these minerals, a linear correlation was also found between cationic exchange capacity (CEC) and specific surface area (S) [5]. As montmorillonite is the soil component, which develops the highest S and CEC, it is suitable to think about its predominance in the correlation mentioned.

The aim of this work was to characterize samples of different bentonite deposits from North Patagonia, Argentina, in order to establish the correlation among the foregoing parameters to predict some of their technological applications.

Samples and techniques

The samples were collected from: Lago Pellegrini (samples 3, 6, 10, 11, 12 and 13) and Río Colorado (samples 1 and 4) of Río Negro province; Zapala (sample 7) and Añelo (samples 2 and 5) of Neuquén province and Puelén (samples 8 and 9) of La Pampa province. All the thirteen samples collected were analyzed by means of the following techniques.

In order to identify the mineral components XRD analyses were carried out by a Rigaku D-MAX-II-C apparatus at 35kV and 15mA, with Cu K_α radiation and Ni filter. Bulk XRD analyses of samples after Green-Kelly test indicated the prevailing presence of dioctahedral smectite, montmorillonite [6-9].

XRD-semiquantitative analyses were performed using characteristic peaks of montmorillonite (4.45 Å), quartz (3.34 Å), feldspar (3.2 Å), calcite (3.04 Å), gypsum (7,6 Å), and zeolite (3.92 Å) [10]. The content of each species was determined upon the ratio of the indicated peak area in the sample with respect to that of the reference (same crystalline species in pure condition) expressed as percentage.

In order to evaluate the clay mineral composition, the <2μm fraction separation was carried out by centrifugation (>10000 rpm) [11].

The specific surface area was determined by adsorption of polar substances as ethylene glycol monoethyl ether (EGME) and water, indicated S_{EGME} and S_W, respectively, as described elsewhere [12-13]. The CEC was determined following the Jackson method [14].

The differential thermal analyses (DTA) were carried out on 200mg sample. The samples were heated in Pt-Ir crucible from room temperature to 1000°C in a Netzsch simultaneous thermal analysis equipment STA 409/c model. The experimental conditions were heating rate, 10°C/min; reference inert material, calcined alumina; DTA sensitivity, 500mV and atmosphere, ambient air.

Mössbauer spectra were taken at room temperature in transmission geometry in a conventional constant acceleration spectrometer of 512 channels with a 50mCi nominal activity ^{57}CoRh source. Spectra were fitted with a non-linear least-squares program with constraints assuming Lorentzian line-shapes. Isomer shifts (δ) are referred to α-Fe at room temperature.

The morphology of particles of some samples was observed by scanning electron microscopy (SEM) using Philips SEM model 505. The analyses were performed on gold sputtered powder samples, following the Goldstein and Muldoon [15] technique. All data obtained were statistically evaluated within 0.01% level of significance [16].

The organic pollutant employed for the adsorption isotherms was a post-harvest fungicide used in the region, the thiabendazole, 2-thiazol-4-yl-benzimidazole, supplied by Chem Service, West Chester, PA (99% purity) and used as received.

For the sorption experiments a weighed amount of thiabendazole was dissolved in absolute ethanol in order to prepare a concentrate solution and further concentrations were obtained by dilution in distilled water. The batch equilibration method was conducted at 20°C, with occasional shaking, in 10ml capped discarding tubes containing a determined montmorillonite suspension and thiabendazole solution without pH adjustment. After the equilibration period of 24h, the supernatant was removed by filtering with µicroclar nitro-cellulose membranes of 0.45µ pore.

Thiabendazole sorptions were determined on the supernatant solutions analysed by UV spectrophotometry (thiabendazole maximum adsorption λ=298nm) using a Hewlett Packard 8453 UV-visible spectrophotometer. The linear range of thiabendazole concentrations was from 2 to 20 mg/L(R^2=0.99). The amount of thiabendazole adsorbed by the montmorillonite (Cs, µmoles thiabendazole/kg clay) was determined as the difference between the initial and the supernatant thiabendazole concentration at the equilibrium (Ce, µmoles thiabendazole/L supernatant solution). All data of isotherms were done by triplicate.

Results and discussion

Mineralogy

Bulk XRD analyses of all samples are shown in Table 1 indicating the prevailing presence of montmorillonite with minor amounts of quartz in all samples and gypsum, feldspar, calcite and zeolite only in some of them.

Clay Fraction

The structural formula was determined following Siguín mathematical calculations [2] from the chemical composition (%) of <2µ fraction presented elsewhere [17]. Table 2 summarizes the tetrahedral (σ) and octahedral (α) substitution, structural formula, S_{EGME}, S_w and CEC. In this table the total octahedral substitution (α) was

differentiated as Fe (ϕ) and Mg (μ) substitutions. These substitutions are also expressed as percentages. The higher Fe content must be pointed out in samples 7 and 13 over the average value obtained from all other samples.

Sample	Mont.	Quartz	Gypsum	Feldspar	Calcite	Zeolite
1	97	<2	<2	<2	<2	0
2	97	<2	2	0	0	0
3	99	<2	0	0	0	0
4	98	<2	<2	0	0	0
5	93	2	1	3	0	1
6	99	<2	0	0	0	<2
7	89	4	0	6	0	1
8	94	2	<2	4	0	0
9	97	<2	0	0	0	2
10	98	<2	0	0	0	2
11	99	<2	<2	0	0	0
12	97	<2	0	0	<2	<2
13	90	7	0	3	0	0

Table 1: *Mineral composition (%) of bulk samples.*

CEC and S values obtained were in agreement with those found in the literature [4,18]. Differences between the values of S_w and S_{EGME} attained for a same sample seem to be related to the tetrahedral substitution degree. The value of S_w is higher or lower than that of S_{EGME} when tetrahedral substitution degree is higher than 0.13 or lower than 0.09, respectively. The high Fe content and the low degree of tetrahedral substitution, of samples 7 and 13 seem also to influence CEC and S values determined for these samples. Particularly, the low CEC values obtained for these samples (7 and 13) seem to indicate a direct influence of the tetrahedral charge, resultant from its isomorphic substitution, on the mineral surface.

As it is known, the thermal stability of montmorillonites is related to the crystalline structure. In particular the loss of OH^- ions causes the structure irreversible modification producing an endothermic peak at 650-700°C [19], in the DTA curve, which indicates the high thermal stability of the sample (T).

Consequently, deformations originated by different isomorphic substitutions will cause a temperature shift of this peak, as was concluded by Siguín et al. [3] ¨the higher degree of octahedral substitution, the lower is the hydroxyl release temperature.

Sample 7 presents two endothermic peaks at 550–686.2°C and sample 13 a single peak at 557.4°C. The low temperature needed for the dehydroxylation, lower than that for the "normal" montmorillonites (700°C [19]), permitted to classify them as "abnormal" ones. This fact can be explained by structure deformations, which increased the layer vulnerability (produced by the high octahedral substitution of iron (Table 2) of samples 7 and 13) and shifted the endothermic peak to lower temperature (Siguín et al.

[3] reported an endothermic peak at 544°C for a bentonite with 0.60 octahedral isomorphic substitution).

Sample	α	ϕ	μ	σ	S_{EGME} (m^2/g)	S_w* (m^2/g)	CEC* (meq/100)
1	0.60	0.21	0.38	0.10	747	778	102
2	0.56	0.23	0.33	0.09	711	705	94
3	0.56	0.29	0.26	0.14	796	866	100
4	0.61	0.23	0.38	0.10	779	738	96
5	0.56	0.20	0.36	0.09	752	689	96
6	0.56	0.28	0.28	0.12	805	792	103
7	0.58	0.37	0.20	0.01	655	659	90
8	0.61	0.23	0.38	0.09	741	724	105
9	0.58	0.18	0.41	0.08	763	732	101
10	0.56	0.28	0.28	0.14	768	843	105
11	0.56	0.27	0.29	0.13	774	814	105
12	0.56	0.23	0.34	0.09	758	726	99
13	0.62	0.32	0.30	0.02	615	556	86

***Table 2**: Tetrahedral (σ), Fe (ϕ) and Mg (μ) octahedral substitutions and total octahedral (α) substitution, structural formula, Specific surface determined by EGME (S_{EGME}) and water (S_w) adsorption and CEC values. (*) Indicated values determined in [27].*

Sample	Structural formula
1	$[(Si_{3.90}Al_{0.10})(Al_{1.40}Fe^{3+}_{0.21}Mg_{0.38})O_{10}(OH)_2]M^{+}_{0.48}$
2	$[(Si_{3.91}Al_{0.09})(Al_{1.44}Fe^{3+}_{0.23}Mg_{0.33})O_{10}(OH)_2]M^{+}_{0.42}$
3	$[(Si_{3.86}Al_{0.14})(Al_{1.44}Fe^{3+}_{0.29}Mg_{0.26})O_{10}(OH)_2]M^{+}_{0.40}$
4	$[(Si_{3.90}Al_{0.10})(Al_{1.39}Fe^{3+}_{0.23}Mg_{0.38})O_{10}(OH)_2]M^{+}_{0.48}$
5	$[(Si_{3.91}Al_{0.09})(Al_{1.44}Fe^{3+}_{0.20}Mg_{0.36})O_{10}(OH)_2]M^{+}_{0.45}$
6	$[(Si_{3.88}Al_{0.12})(Al_{1.44}Fe^{3+}_{0.28}Mg_{0.28})O_{10}(OH)_2]M^{+}_{0.40}$
7	$[(Si_{3.99}Al_{0.01})(Al_{1.42}Fe^{3+}_{0.37}Mg_{0.20})O_{10}(OH)_2]M^{+}_{0.21}$
8	$[(Si_{3.91}Al_{0.09})(Al_{1.39}Fe^{3+}_{0.23}Mg_{0.38})O_{10}(OH)_2]M^{+}_{0.47}$
9	$[(Si_{3.92}Al_{0.08})(Al_{1.42}Fe^{3+}_{0.18}Mg_{0.41})O_{10}(OH)_2]M^{+}_{0.49}$
10	$[(Si_{3.86}Al_{0.14})(Al_{1.44}Fe^{3+}_{0.28}Mg_{0.28})O_{10}(OH)_2]M^{+}_{0.42}$
11	$[(Si_{3.87}Al_{0.13})(Al_{1.44}Fe^{3+}_{0.27}Mg_{0.29})O_{10}(OH)_2]M^{+}_{0.42}$
12	$[(Si_{3.91}Al_{0.09})(Al_{1.44}Fe^{3+}_{0.23}Mg_{0.34})O_{10}(OH)_2]M^{+}_{0.43}$
13	$[(Si_{3.98}Al_{0.02})(Al_{1.38}Fe^{3+}_{0.32}Mg_{0.30})O_{10}(OH)_2]M^{+}_{0.32}$

***Table 2, cont**.: Tetrahedral (σ), Fe (ϕ) and Mg (μ) octahedral substitutions and total octahedral (α) substitution, structural formula.*

Figure 1 shows the DTA curves and T obtained for all samples.

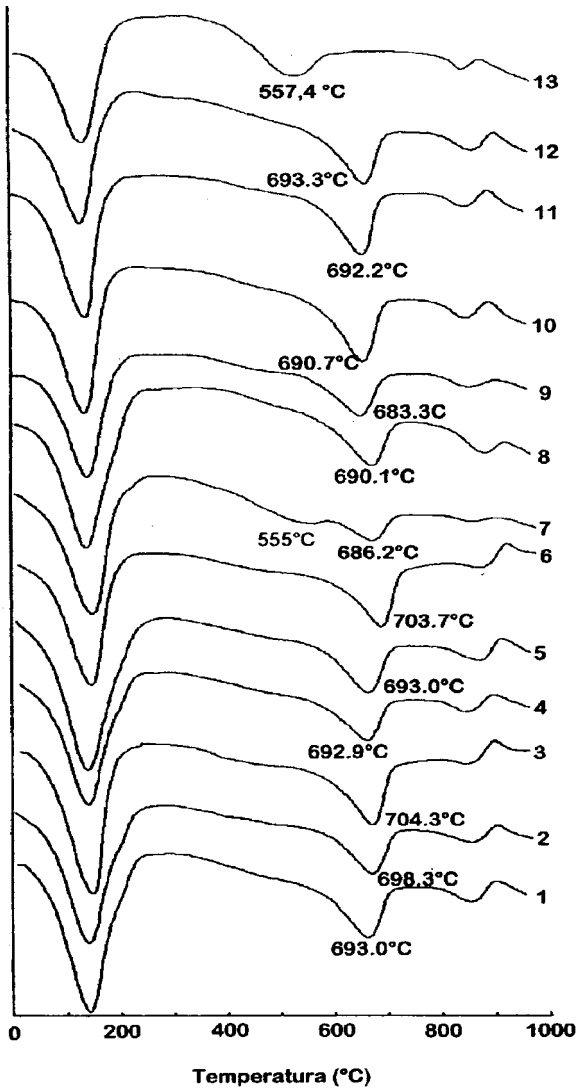

Figure 1: *DTA curves for all samples.*

1. Octahedral and Total isomorphic substitutions

Correlation analyses of octahedral ($\alpha\% = \phi\% + \mu\%$) and total ($\gamma\% = \alpha\% + \sigma\%$) isomorphic substitution degrees with S_{EGME}, S_w, T and CEC were determined.

Statistical correlation analysis of both (octahedral and total) isomorphic substitution degrees versus S, CEC and T values, respectively, indicated no correlation with a linear mathematical model (R^2 coefficients for all correlations were <0.40).

The amount and coordination state of iron substituting Al^{3+} in the octahedral layer could be one way to explain the low correlation coefficients obtained. The amount of iron substitution related to the coordination state would produce structure distortions because

the difference of ionic size from that of Al^{3+} (Pauling ionic ratio Al^{+3}= 0.5; Fe^{+3}= 0.64; Fe^{+2}=0.75Å) [20], thus Fe^{+2} generates the most important difference.

The coordination state of iron was determined by Mössbauer spectroscopy in samples with iron substitution of low, intermediate and high degree (samples 13, 12 and 9, respectively). The values of Fe^{+2}/Fe^{+3} ratio obtained were 0.12, 0.17 and 0.25, for samples 13, 12 and 9, respectively. These values indicated a minor presence of low coordination iron (Fe^{+2}) producing a neglected excess of negative charge and structure distortion, which can explain the low correlation coefficient (R^2<0.40) obtained.

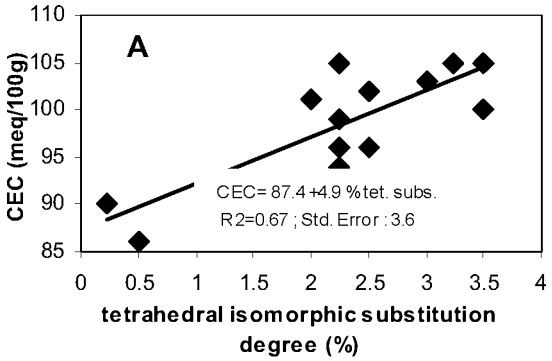

Figure 2a: *Linear regression models for CEC as a function of tetrahedral isomorphic substitution degree.*

On the other hand, Siguín et al. [3] found a polynomial regression (T= 785 - 5α) with a correlation coefficient R^2=0.948, for octahedral isomorphic substitution degree and T. The series of samples used ranged a wider α (between 0.33 and 0.89) than that of samples studied in this work (Table 2), which could explain the low correlation coefficient found in this study. It is important to indicate that a better refinement of the polynomial regression was obtained by Siguín et al. [3] after elimination of points where iron and magnesium contents were much higher than those of the cation concerned. This fact produced a change in the intercept point from 785 to 731°C, which agrees with the intercept point found for data of this study (757°C). The intercept temperature value reported for zero substitution (pyrophyllite) is 800°C, the value obtained in this work and those reported by Siguín et al. [3] are somewhat lower than that of pyrophyllite and reflect the simultaneous influence of ferric and magnesium ions.

In this study, although the octahedral isomorphic substitution degree was higher than the tetrahedral one (Table 2), the simultaneous influence of octahedral substituents (ferric and magnesium ions) would produce the appearance of not directly influencing the surface structure behavior.

2. Tetrahedral isomorphic substitution

Figure 2a-d show the mathematical linear regression models for CEC, S_{EGME}, $S_{w.}$, and T, respectively, as a function of tetrahedral substitution degree for all samples.

The linear regression model found for CEC-tetrahedral isomorphic substitution degree (σ %) (Figure 2 A) was attributed to changes in the reactivity of the siloxan

cavity. Particularly, the isomorphic substitution of Si^{4+} by Al^{3+} in the tetrahedral layer produces a net positive charge deficit, which would strengthen the bond and consequently the reactivity of this layer with interlayer cations more than the excess of negative charge produced by octahedral substitutions, due to the far location of the octahedral layer [21]. The excess of negative charge found in the tetrahedral layer also affects polar molecules as water and EGME that will replace interlayer cations to measure the surface.

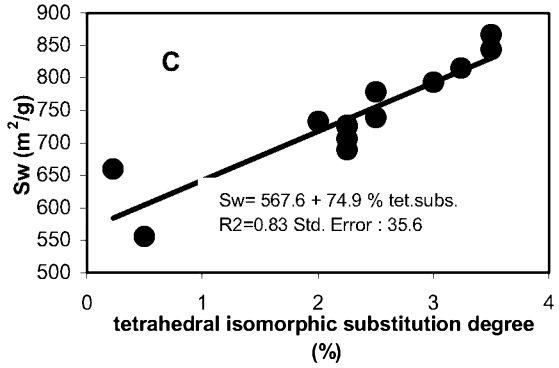

Figure 2b: *Linear regression models for S_{EGME} as a function of tetrahedral isomorphic substitution degree.*

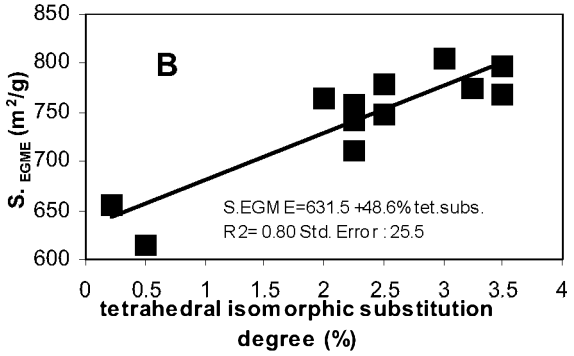

Figure 2c: *Linear regression models for S_w as a function of tetrahedral isomorphic substitution degree.*

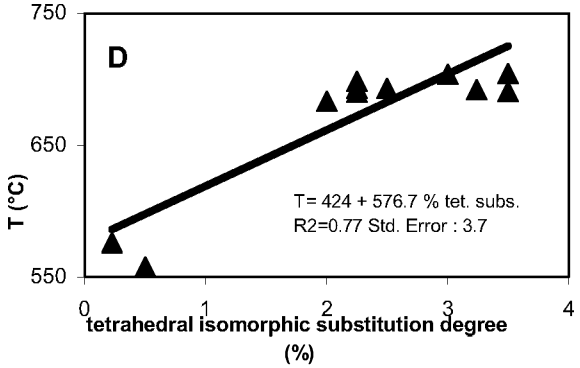

Figure 2d: *Linear regression models for T as a function of tetrahedral isomorphic substitution degree.*

The difference between correlations of specific surface area values obtained by both methods and the isomorphic tetrahedral substitutions (Figures 2 B and C) is related to the interlayer charge and can be attributed to the following facts. In the EGME method, the surface adsorption can go with coating, by the same mechanisms used by water in hydrated systems [22]. In the case of water, the adsorption was mainly produced by surface ionic solvation, consequently small water amount was adsorbed out of the interlayer space [23]. This fact produced the increase observed (Table 2) in the S_w value respect to that obtained with EGME method, for samples with isomorphic tetrahedral substitution value higher than 0.13.

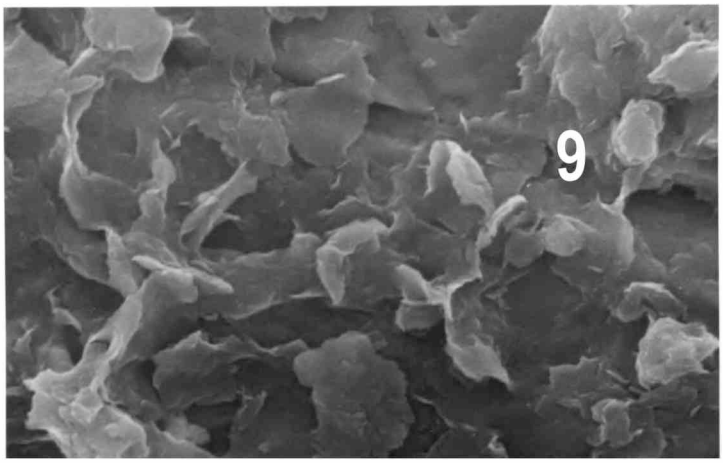

Figure 3: *SEM micrographs of samples 9, 11 and 12 at same magnification.*

The correlation between T and tetrahedral substitution degree (Figure 2 D), in agreement with that obtained by Siguin et al. [3], for T and octahedral substitution degree (over a series of bentonites with Fe^{3+} substitution degree between 5.5 and 30.0) indicates that the increase of tetrahedral substitutions promotes an increase in the amount of exchangeable cations which at the same time preserves the layer and stabilizes the structure [24-25].

Figure 3 shows SEM micrographs of samples with different tetrahedral and same octahedral substitution degrees, samples 11 and 12 of Lago Pellegrini deposit and sample 9 of Puelén deposit with lower tetrahedral and higher octahedral substitution degrees than prior samples. In spite of the similar physicochemical parameter values of the three samples (Table 2), SEM micrographs showed rather uniform and random packing particles for all samples observed. Notwithstanding, different particle association was found among them, mainly produced in the surface charges originated during the water dispersion for the microscopy sample preparation. Samples with high tetrahedral substitutions, due to the TOT (tetrahedral – octahedral – tetrahedral) arrangement of montmorillonite, will indicate a negative charge of face surface (compensated by the interlayer cations) and the existence of high octahedral substitutions will indicate a

positive charge of edge surface [26] (only compensated by the H^+ or OH^- ions of the solution).

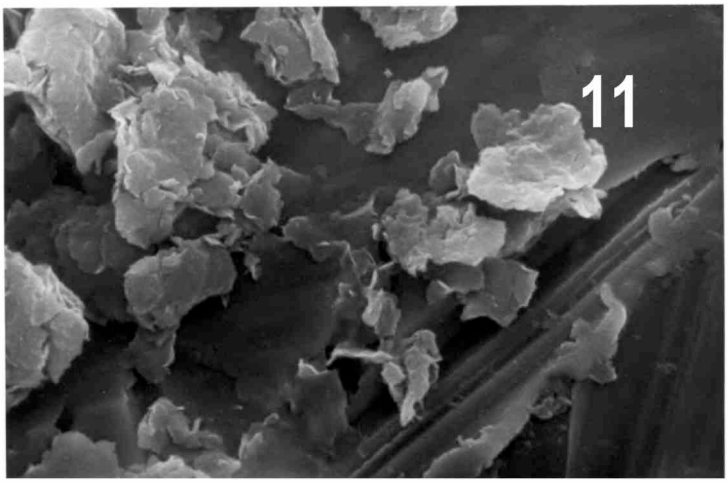

Figure 3, cont.: *SEM micrographs of samples 9, 11 and 12 at same magnification.*

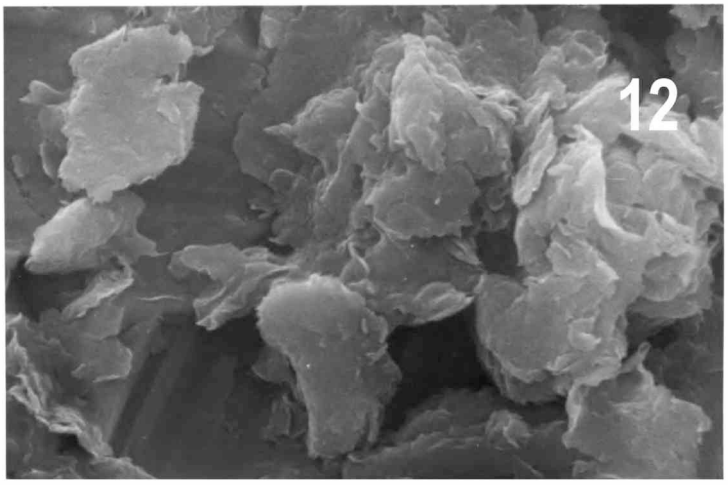

Figure 3, cont.: *SEM micrographs of samples 9, 11 and 12 at same magnification.*

Sample 9 shows the particle mostly associated according to the edge-to-edge mode, in agreement with its high octahedral and low tetrahedral substitutions. Sample 11 shows a face-to-face predominant mode, also in agreement with the inverse isomorphic substitution degrees of this sample respect to sample 9 and highest tetrahedral substitution value of this sample among the other samples. Sample 12 showed an intermediate association behavior as expected from its substitution degree values

Bentonites

In bentonite bulk samples (data not shown), as it happens with <2μm fractions, little or no correlation was found among S_{EGME}, S_{w}., CEC and T and octahedral or total isomorphic substitution degrees. These samples also follow the same trend as that of <2μm fraction with the tetrahedral isomorphic substitution degree. A mathematical model could not be found due to the low R^2 obtained (R^2=0.38 and 0.30 for CEC and S respectively). However a linear regression model between T and tetrahedral isomorphic substitution with R^2=0.74 was found, similar to that obtained for <2μm fractions.

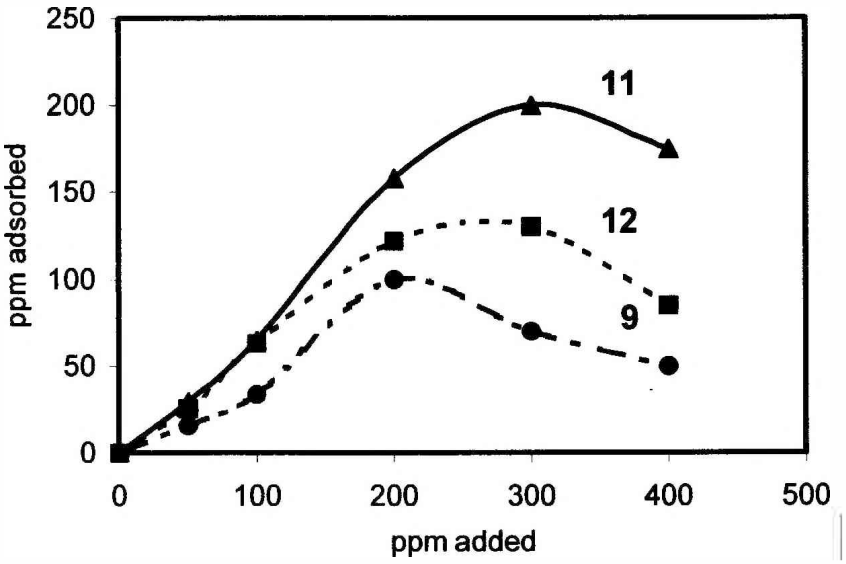

***Figure 4**: Fungicide adsorption curves for samples 9, 11 and 12.*

Applications

Some bulk bentonite samples of North Patagonia were already used as raw material for foundry sands, drilling mud and bleaching earth [6]. The preceding sample characterization indicates that some of them can be used also for organic pollutant adsorption.

Deposit proximity (Lago Pellegrini) to the packing plants was the first selection factor to choose samples, 11 and 12, for a post-harvest fungicide (thiabendazole) adsorption. Sample 9 with low tetrahedral substitution degree and high purity of the clay mineral, from different deposit (Puelén) was also selected to determine the fungicide adsorption isotherms.

Adsorption isotherms were determined at the optimum adsorption parameters, room temperature, pH (5-7), contact time (12h) and adsorbent/adsorbate ratio (1000 mg/l) determined elsewhere [27] using batch equilibration. The higher affinity from organic than ionic molecules of montmorillonite surface [28] led to neglect the solvent competence in the adsorption isotherms. Figure 4 shows the fungicide adsorption curves for samples 9, 11 and 12.

Figure 4 indicates that sample 11 adsorbed larger amount of fungicide than samples 9 and 12. The high tetrahedral substitution degree (σ %), which correlates linearly with CEC, S_w and face to face predominant particle association of this sample seems to favor the fungicide adsorption.

Conclusions

S_{EGME}, S_{w}., CEC and T are linearly correlated with tetrahedral isomorphic substitution degree for montmorillonites from North Patagonia. Further technological applications of these minerals could be evaluated with the obtained mathematical models.

This characterization of samples and the established mathematical models allowed anticipating the best adsorptive sample for an organic pollutant (thiabendazole, fungicide) as those of high tetrahedral isomorphic substitution.

Acknowledgments

Authors thank Professor R. Mercader for the Mössbauer iron determination and S. Conconi for the Thermal analysis. Financial support provided by Universidad Nacional del Comahue and CONICET (PIP 217/98) is gratefully acknowledged.

References

[1] Siguín, D.; Ferreira, S; Foufre, L.; García, F. *J. Mater. Sci.* **1993**, *28*, 6163.
[2] Siguín, D.; Ferreira, S.; Foufre, L.; García, F. *J. Mater. Sci.* **1994**, *29*, 4379.
[3] Siguín, D.; Ferreira, S.; Foufre, L.; García, F. *J. Amer. Ceram. Soc.* **1995**, *78*, 2215.
[4] Torres Sánchez, R.M. *J. Coll. and Surf.* **1997**, *127*, 134.
[5] Newman, A. *J. Soil Sci.* **1983**, *34*, 23.
[6] Vallés, J.M.; Impiccini, A. *Instituto de Geología y Recursos Minerales SEGEMAR, Anales* **1999**, *35*: 1113 and **1999**, *35*: 1385.
[7] Impiccini, A. *In Mineralogía de la fracción no arcillosa de las bentonitas del Cretácico superior de la región Norpatagonia*. PhD Thesis UNLP (**1995**).
[8] Iñíguez Rodríguez, A.M.; Andreis, R.R.; Lluch, J.J. Unpublished (**1972**).
[9] Vallés, J.M.; Burlando, L.; Chiachiarini, P.; Giaveno, M.A.; Impiccini, A. *In P.I.C.G.-24. Cretácico de América Latina*, Buenos Aires. **1989**, p 79.
[10] Dixon, J.; Weed, S. *In Minerals in Soil Environments*. Soil Science Society of America. **1977**, p 89.
[11] Galehouse, J. *In Procedures in Sedimentary Petrology*, (Carver, R. ed.) John Wiley & Sons, **1971**, p 69.
[12] Heilman, M.; Carter, D.; Gonzáles, C. *Soil Sci.* **1965**, *100*, 409.
[13] Lombardi, B.; Baschini, M.; Torres Sánchez, R.M. *In New Trends in Mineral Processing III*, **1999**, p 339.
[14] Jackson, M.L. *In: Análisis Químico de Suelos*, Omega, 3ra. ed., Barcelona. **1976**.
[15] Goldstein, J.; Muldoon, J. *In Electron and ion probe microanalysis*. Plenum Press, **1977**.
[16] Montgomery, D. *In Diseño y análisis de experimentos*. Iberoamericana. **1991**.
[17] Lombardi, B.; Baschini, M.; Torres Sánchez, R.M. **2002**, accepted in *Appl. Clay Min.*

[18] Newman, A. *In Chemistry of Clays and Clay Minerals*. Chap. 5 Mineralogical Soc. (Newman, A. ed.), **1987**, p 257.
[19] Sudo, T.; Shimada, S. *In Differential thermal analysis*. (Mackenzie, R. ed.). Academic Press, **1970**, p 539.
[20] Ball, M.; Norbury, A. *In Phys. Data Inorg. Chem.* **1974**, 133.
[21] Sposito, G. *In Surface chemistry of soils*. Oxford University Press, **1984**, pp 26, 30.
[22] Carter, D.; Mortland, M.; Kemper, W. *In Methods of Soil Analysis, Part I. Physical and Mineralogical Methods*. Agronomy Monograph Nº 9 (2nd Edition), **1986**, p 413.
[23] Prost, R.; Koutit, T.; Benchara, A.; Huard, E. *Clays and Clay Min*. **1998**, *46*, 117.
[24] Drits, V.; Manceau, A. *Clays and Clay Minerals*, **2000**, *48*, 185.
[25] Vallés, J.M.; Giaveno, M.A. *XII Congreso Geológico Argentino. V*. **1993**, p 262.
[26] Van Olphen, H. *In Clay Colloid Chemistry*. John Wiley & Sons, **1977**, p. 236.
[27] Lombardi, B.; Baschini, M.; Torres Sánchez, R.M. **2002**, (submitted to Applied Clays).
[28] Lagaly, G. *Prog. Coll. and Polym. Sci*. **1999**, *497*, 137.